Observer-Based Integral Sliding Mode Controller for a Two-Wheeled Inverted Pendulum

Ravindra K. Munje[1†], **Ranvir J. Desai**[2], and **Balasaheb M. Patre**[2], Non-members

ABSTRACT

The modeling and control of a two-wheeled inverted pendulum (TWIP) is gaining much interest due to the various advancements in hardware and computing technologies. A TWIP system has many advantages and applications. However, it still faces many challenges such as positioning, disturbance rejection, parameter uncertainties, etc. In this paper, a control scheme based on modern control techniques is presented to overcome these issues. Furthermore, an observer-based robust integral sliding mode controller (ISMC) is proposed for the nonlinear TWIP system. Firstly, a robust integral sliding mode controller is designed to tackle short-term and long-term constant and time-varying disturbances as well as issues relating to parameter variation. Secondly, the reduced-order observer is designed to estimate immeasurable states, enabling simplified implementation. It is then applied to the nonlinear model of the TWIP system, and performance is observed under different transient conditions. A comparison with prevalent controllers in the literature is carried out. This comparison relates to graphical results, time domain specifications, and error performance indices, calculated for states. From this, a significant qualitative improvement can be observed with the proposed controller for all types of transients. In quantitative terms, zero steady-state error with disturbances and a five-fold improvement in settling time with parameter variations are observed. This paper also discusses the software Simulink realization for modeling and control of the TWIP system, which can be valuable for novices working in this area.

Keywords: Integral Sliding Mode, Observer-Based Control, Simulink Modeling, Sliding Mode Control, Two-Wheeled Inverted Pendulum, TWIP

1. INTRODUCTION

The two-wheeled inverted pendulum (TWIP) is a highly nonlinear and naturally unstable system. It is an underactuated system with three degrees of freedom consisting of pitch, yaw, and straight-line movements merely with two wheels [1]. This interesting system has attracted the attention of many researchers worldwide over the last three decades. However, there are some challenges with this system such as mathematical modeling, controller design, and implementation. Although the modeling is difficult due to nonlinear and complex dynamics, uncertain environmental conditions, parameter uncertainties, etc., several research groups have proposed mathematical models for the TWIP system.

In [2], an exact and accurate nonlinear model of the TWIP system is proposed which overcomes the drawbacks of earlier models, such as inappropriate assumptions, improper terms, and the omission of some important terms, etc. The control design of this system also plays an important role. In the literature, the controllers for the TWIP system are designed using the linear quadratic regulator (LQR) [3], feedback linearization [4], fuzzy logic [5, 6], sliding mode control [7], and optimal control [8], etc.

In [9], the gray box modeling of a TWIP robot using the Lagrange equation is proposed, in which a closed-loop parameter identification method is used. Furthermore, in this paper, the design and software implementations of PID and LQR are demonstrated. In another study, the model of TWIP is obtained using differential equations, and then PID, LQR, and linear quadratic Gaussian (LQG) controllers are designed. The performance of LQG is shown to be superior to LQR [10].

In [11], an optimal controller based on model predictive control is designed to demonstrate the performance improvement over PID for the self-balancing two-wheeled robot system. In [12], an integral sliding mode controller (ISMC) is designed and the performance is compared with [11]. However, disturbance is not considered in this case. Nevertheless, in all the above designs, the 4th order model is used to design the controller, i.e., yaw motion dynamics are not considered.

In [13], the Newton-Euler method is used to derive a mathematical model of the two-wheeled self-balancing robot. The LQR is designed for the linear system and the influence of $\boldsymbol{Q}$ and $\boldsymbol{R}$ on the system state is analyzed. For implementing state feedback-based controllers like LQR, information on states is required. In [14], a Luenberger observer is used to estimate the unmeasured states, and

Manuscript received on January 29, 2022; revised on July 18, 2022; accepted on September 26, 2022. This paper was recommended by Associate Editor Matheepot Phattanasak.

[1]The author is with the Department of Electrical Engineering, K. K. Wagh Institute of Engineering Education and Research, Nashik, India.

[2]The authors are with the Department of Instrumentation Engineering, Shri Guru Gobind Singhji Institute of Engineering and Technology, Nanded, India.

[†]Corresponding author: ravimunje@yahoo.co.in

Digital Object Identifier: 10.37936/ecti-eec.2023211.248610

the LQR controller is then established. Very recently, an underactuated sliding mode control scheme has been implemented using a variety of control parameters [15]. The controller performance is successfully tested for set-point changes and disturbance conditions using MATLAB simulation.

In [16], the controller is designed to keep the TWIP in an upright position, preventing it from tipping over when the TWIP is subjected to either unexpected impulses or shifting weights along with its chassis. In [17], different controllers are tested for an inverted pendulum system. In this work, LQR, pole placement, and PID are designed for the simulation. Nonetheless, the control designs discussed so far are applied to linearized models of the TWIP. In [18], a fractional-order PID controller is designed for a mobile robot. However, limited simulation cases are discussed.

From the literature review, it can be observed that the development of an accurate mathematical model and the design of the control algorithm for asymptotic stabilization in the presence of a disturbance environment are tedious tasks for the TWIP system. Some controllers work well for steady disturbances and others for dynamic disturbances. Very few controllers are available for alleviating both disturbance situations. Furthermore, most of the controls are designed assuming the availability of the states for measurement. However, it is impractical or sometimes expensive to measure some of the states, e.g., time derivatives of measurable states. In such a situation either a full- or reduced-order observer would be more useful.

In this paper, the design of an observer-based integral sliding mode controller for a TWIP system is proposed to achieve steady-state and transient performance. The transient performance of the said system is examined using all types of disturbances. The main contributions of the paper are as follows.

1) Designing an integral sliding mode controller for achieving both an acceptable steady-state and transient performance. Here, the transient performance is tested for disturbances like constant (temporary and continuous) steps, sinusoidal (time-varying) disturbances, and parameter variations.
2) Designing a reduced-order observer for the system to estimate immeasurable states.
3) Demonstrating the applicability of the proposed control scheme on the 6th-order nonlinear model of the TWIP system with realizable Simulink blocks.

To show the effectiveness of the suggested controller the simulation results are compared with an existing controller. This includes a comparison based on simulation graphs (qualitative) and error performance indices (quantitative) calculated for outputs.

The remainder of the paper is organized as follows. In Section 2, the nonlinear mathematical model of the TWIP is discussed. In Section 3, the design of an integral sliding mode controller is presented. Section 4 discusses the reduced-order observer design. The simulation results and discussions are presented in Section 5. Finally, the paper is concluded in Section 6.

2. DYNAMIC MODEL OF A TWIP SYSTEM

A comprehensive mathematical model of TWIP has been proposed in [2, 8]. The same model is used here for exploring the possibility of an observer-based integral sliding mode controller. This model is given by the following nonlinear equations:

$$\dot{x}_1 = x_2 \tag{1}$$
$$\dot{x}_2 = a_2(x)\,x_3 + b_2(x)\left(T_L + T_R\right) \tag{2}$$
$$\dot{x}_3 = x_4 \tag{3}$$
$$\dot{x}_4 = a_4(x)\,x_3 + b_4(x)\left(T_L + T_R\right) \tag{4}$$
$$\dot{x}_5 = x_6 \tag{5}$$
$$\dot{x}_6 = a_6(x)\,x_3 + b_6(x)\left(T_L - T_R\right) \tag{6}$$

where x_1, x_3 and x_5 are respectively straight, pitch (θ), and yaw (ψ) motions and x_2, x_4 and x_6 are corresponding time derivatives. This system is of the 6th order with two inputs T_L and T_R, i.e., torques applied to the left and right wheels respectively. The functions $a_i(x)$ and $b_i(x)$, in Eqs. (1)–(6), are given by the following equations.

$$a_2(x) = \frac{1}{\eta_1(x_3)}\frac{\sin x_3}{x_3}\left[p_5\cos x_3 + p_6x_4^2 + p_7x_6^2 + p_8\cos^2 x_3x_6^2\right] \tag{7}$$

$$a_4(x) = \frac{1}{\eta_1(x_3)}\frac{\sin x_3}{x_3}\left[p_9 + p_{10}x_4^2\cos x_3 + p_{11}\cos x_3x_6^2\right] \tag{8}$$

$$a_6(x) = \frac{1}{\eta_2(x_3)}\frac{\sin x_3}{x_3}\left[p_{12}x_4x_6\cos x_3 + p_{13}x_2x_6\right] \tag{9}$$

$$b_2(x) = \frac{1}{\eta_1(x_3)}\left[p_{14}\cos x_3 + p_{15}\right] \tag{10}$$

$$b_4(x) = \frac{1}{\eta_1(x_3)}\left[p_{16}\cos x_3 + p_{17}\right] \tag{11}$$

$$b_6(x) = \frac{1}{\eta_2(x_3)}\left[p_{18}\right] \tag{12}$$

$$\text{with}\quad \eta_1\left(x_3\right) = \left[p_1 + p_2\sin^2 x_3\right] \tag{13}$$

$$\eta_2\left(x_3\right) = \left[p_3 + p_4\sin^2 x_3\right] \tag{14}$$

where p_i's and other parameters are given as follows:

$$p_1 = m_BI_2 + 2\left(m_W + \left(J/r^2\right)\right)\left(I_2 + m_Bl^2\right) \tag{15}$$
$$p_2 = \left(m_Bl\right)^2 \tag{16}$$
$$p_3 = I_3 + 2J_v + 2\left(m_W + \left(J/r^2\right)\right)d^2 \tag{17}$$
$$p_4 = I_1 + m_Bl^2 - I_3 \tag{18}$$

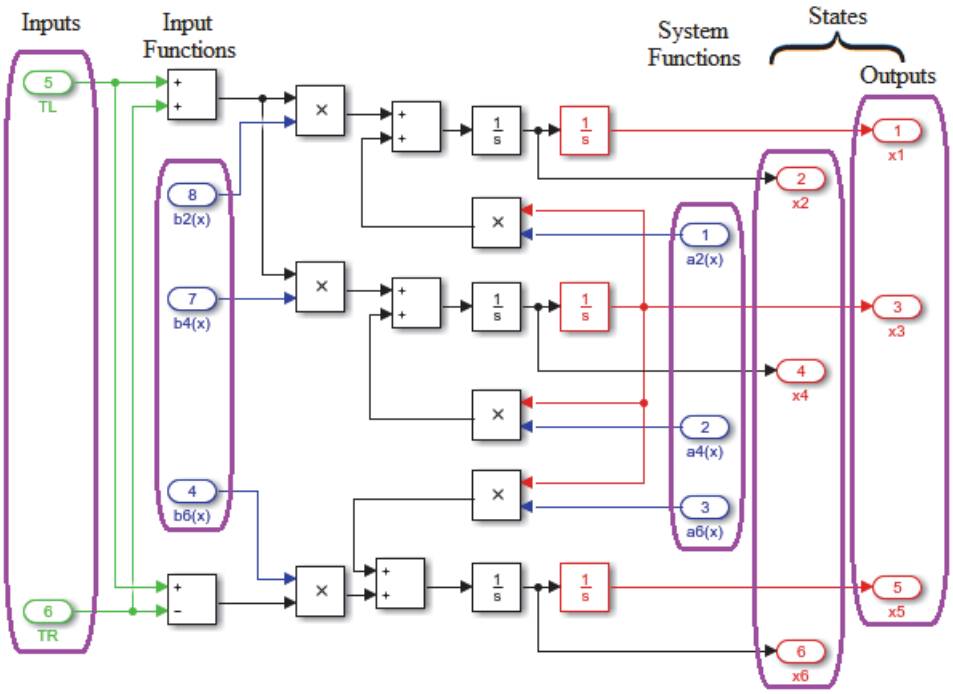

***Fig. 1**: Nonlinear Simulink model of the TWIP system.*

$$p_5 = -\left(m_B l\right)^2 g \tag{19}$$

$$p_6 = \left(I_2 + m_B l^2\right) m_B l \tag{20}$$

$$p_7 = m_B l I_2 + m_B^2 l^3 \tag{21}$$

$$p_8 = m_B l \left(I_3 - I_1 - m_B l^2\right) \tag{22}$$

$$p_9 = \left(m_B + 2m_W + 2\left(J/r^2\right)\right)\left(m_B l g\right) \tag{23}$$

$$p_{10} = -p_2 \tag{24}$$

$$p_{11} = -\Big[\left(m_B l\right)^2 + \left(I_3 - I_1 - m_B l^2\right) \cdot \left(m_B + 2m_W + 2\left(J/r^2\right)\right)\Big] \tag{25}$$

$$p_{12} = 2\left(I_3 - I_1 - m_B l^2\right) \tag{26}$$

$$p_{13} = -m_B l \tag{27}$$

$$p_{14} = -p_{13} \tag{28}$$

$$p_{15} = \left(I_2 + m_B l^2\right)/r \tag{29}$$

$$p_{16} = -p_{13}/r \tag{30}$$

$$p_{17} = m_B + 2m_W + 2\left(J/r^2\right) \tag{31}$$

$$p_{18} = -d/r \tag{32}$$

All p_i's are constants, calculated from the system parameters. The values of all parameters in p_i with their meanings are given in Table 1. Eqs. (1)–(6) are linearized using the Taylor series approximation. The steady-state values and inputs are taken as zero and then represented in the standard state-space form as

$$\dot{x} = Ax + Bu \tag{33}$$

$$y = Cx \tag{34}$$

with the state, input, and output vectors as

$$x = [x_1 \;\; x_2 \;\; x_3 \;\; x_4 \;\; x_5 \;\; x_6]^T \tag{35}$$

$$u = [T_L \;\; T_R]^T \tag{36}$$

$$y = [x_1 \;\; x_3 \;\; x_5]^T \tag{37}$$

The eigenvalues of Eq. (33) are found to be (–5.2267, 0, 0, 0, 0, 5.2267), i.e., the system is open-loop unstable, but found to be observable and controllable. Controllability and observability play important roles in controller and observer designs, respectively. Responses for the input conditions are zero for both linear and nonlinear models.

The purpose of linearizing the nonlinear TWIP system is three-fold: (i) to show that the linearized system adequately represents the nonlinear system, (ii) to examine properties like controllability, observability, and stability of the system, and (iii) to design controllers based on a linear model, since it satisfactorily resembles a nonlinear system. It must be noted that, despite the controller and observer being designed using a linear model, they are tested on the nonlinear system developed in MATLAB Simulink [19] as shown in Fig. 1.

In Fig. 1, only the final subsystem (realization of Eqs. (1)–(6)) is shown with clear indications for inputs (T_L and T_R), input functions ($b_i(x)$), system functions ($a_i(x)$), outputs (x_1, x_3, x_5), and states (x_1 to x_6). Other subsystems of input and system functions are not shown. These subsystems can be developed in the same way as that presented in Fig. 1 using Eqs. (7)–(14) and values in Table 1.

In the following sections, initially, an integral sliding mode controller (ISMC) is designed, and then implemented using a reduced-order observer.

***Table 1**: Parameter values for the TWIP system [8].*

Symbols	Meaning of symbols	Values
d	Distance between wheels	0.6 m
m_B	Mass of pendulum body	45 kg
m_W	Mass of wheel	2 kg
l	Length of the pendulum rod	0.135 m
r	Radius of wheels	0.2032 m
I_1	Moment of inertia of pendulum body for b_1	1.9 kg·m^2
I_2	Moment of inertia of pendulum body for b_2	2.1 kg·m^2
I_3	Moment of inertia of pendulum body for b_3	1.6 kg·m^2
J	Moment of inertia of a wheel for the wheel axis	0.02 kg·m^2
J_v	Moment of inertia of a wheel for the vertical axis	0.04 kg·m^2
g	Acceleration due to gravity	9.81 m/s^2

3. ROBUST INTEGRAL SLIDING MODE CONTROLLER

Let us consider a linear system with parametric uncertainties, unmodeled dynamics, and external disturbances, represented as

$$\dot{x}(t) = (A + \Delta A)\, x(t) + (B + \Delta B)\, u(t) + \xi(t) \tag{38}$$

$$y(t) = Cx(t) \tag{39}$$

where $x \in R^n$ is the state, $u \in R^m$ is input and $y \in R^p$ is output. A, B, and C are the known real constant matrices with appropriate dimensions. Furthermore, ΔA and ΔB are parametric uncertainties and $\xi(t)$ represents the uncertainty due to unmodeled dynamics and external disturbances affecting the system. The following assumptions are made.

Assumption 1: The system (A, B, C) is controllable and observable.

Assumption 2: Parametric uncertainties, unmodeled dynamics, and external disturbances are unknown but bounded and satisfy the matching condition, i.e. $\xi(t) \in span(B)$.

From Assumption 2, let the system uncertainties be written as

$$\Delta Ax(t) + \Delta Bu(t) + \xi(t) = BD\xi(t) \tag{40}$$

where $\xi(t) \in R^l$ and $D \in R^{m\,x\,l}$. With Eq. (40), the system Eq. (38) can be written as

$$\dot{x}(t) = Ax(t) + B(u(t) + D\xi(t)) \tag{41}$$

The objective is to design a robust controller Eq. (41), such that the system becomes insensitive to uncertainties and external disturbances. Let us assume that the control input $u(t)$ has two parts, i.e., a continuous part and a discontinuous part defined as

$$u(t) = u_c(t) + u_d(t) \tag{42}$$

where $u_c(t)$ is the continuous control and $u_d(t)$ is the discontinuous control. Using Eq. (42), Eq. (41) becomes

$$\dot{x}(t) = Ax(t) + B(u_c(t) + u_d(t) + D\xi(t)) \tag{43}$$

In this, the continuous control $u_c(t)$ is designed using the eigenvalue assignment technique, and the discontinuous control $u_d(t)$ designed using the ISMC technique [20].

3.1 Design of Continuous Control

Continuous control $u_c(t)$ is designed for a nominal system. Hence, by neglecting the uncertain part in Eq. (43) one can get a nominal system as

$$\dot{x}(t) = Ax(t) + Bu_c(t) \tag{44}$$

In this, the control input is given by

$$u_c(t) = -Kx(t) \tag{45}$$

where $K \in R^{m\,x\,n}$ is a state feedback gain matrix, designed such that $\lambda_{desired} = \lambda(A - BK)$, where $\lambda(\cdot)$ are eigenvalues of the system and $\lambda_{desired}$ the desired eigenvalues. It must be noted that the controller Eq. (45) may not be able to control the uncertain system Eq. (43) directly. To address the uncertainties present in the system, the controller is required to be combined with ISMC to guarantee robustness throughout the motion.

3.2 Design of Discontinuous Control

Let us define the sliding surface as

$$s(t) = Gx(t) + z(t) \tag{46}$$

where $G \in R^{m\,x\,n}$ provides freedom to the designer and $z(t) \in R^m$ induces the integral term. During sliding, $s(t) = \dot{s}(t) = 0$ and, therefore, from Eq. (46)

$$\dot{s}(t) = G\dot{x}(t) + \dot{z}(t) = 0 \tag{47}$$

Substituting $\dot{x}(t)$ from Eq. (43) in Eq. (47) and compensating matched uncertainty, i.e., $(u_d(t))_{eq} = -D\xi(t)$ one can obtain

$$\dot{z}(t) = -G(Ax(t) + Bu_c(t)) \tag{48}$$

Integrating Eq. (48) gives $z(t)$. Substituting this in Eq. (46) with initial condition $z(0) = -Gx(0)$ gives

$$s(t) = Gx(t) - Gx(0) - G\int_0^t \left(Ax(\tau) + Bu_c(\tau)\right) d\tau \tag{49}$$

where G is chosen as the left pseudo-inverse of B, making GB invertible and ensuring $-Gx(0)$ makes $s(0) = 0$, thereby eliminating the reaching phase. This choice of G reduces the amplitude of chattering [21]. The discontinuous control $u_d(t)$ is designed based on exponential reaching law [22] as

$$u_d(t) = -(GB)^{-1}(\mu\,\mathrm{sgn}(s(t)) + ks(t)) \tag{50}$$

where μ is constant with $\mu > 0$.

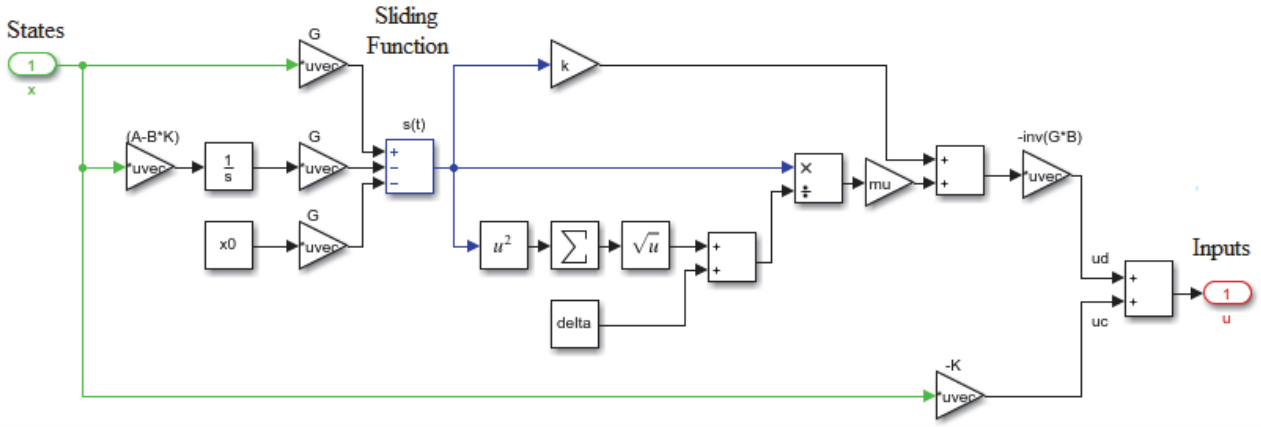

Fig. 2: Simulink model of ISMC signal generation.

From Eqs. (42), (45), and (50), the control law $u(t)$ is given as

$$u(t) = -Kx(t) - (GB)^{-1}\left(\mu \operatorname{sgn}(s(t)) + ks(t)\right) \tag{51}$$

Chattering is overcome by using a boundary layer technique where the sgn(·) function is replaced by $s/(|s| + \delta)$. In this, δ is a small positive design scalar. Using Eq. (51), a practical control law is obtained as

$$u(t) = -Kx(t) - (GB)^{-1}\left(\mu \frac{s(t)}{|s(t)| + \delta} + ks(t)\right) \tag{52}$$

The MATLAB implementation of Eq. (52) is illustrated in Fig. 2. All the states of the system (either actual, shown in Fig. 1, or estimated, discussed in the next section) are the inputs to Fig. 2 and the output is the control signal Eq. (52). This control signal is fed back to the inputs in Fig. 1.

In the next section, the reduced-order observer design is presented for the realization of the controller discussed in this section.

4. REDUCED-ORDER OBSERVER DESIGN

Considering the nominal part of the system Eq. (38), given by Eq. (44), and the output Eq. (39), let us assume that p number of states (outputs) are available for direct measurement. Therefore, it is necessary to estimate $r = n - p$ states, which are immeasurable. The order of the reduced-order observer is r. The design of the reduced-order observer is taken from [23].

Considering an arbitrary matrix C_1 of dimension $r \times n$ whose rank is equal to $r = n - p$ such that rank $\begin{bmatrix} C & C_1 \end{bmatrix}^T = n$. Introducing vector y_1 of dimension r as

$$y_1 = C_1 x \tag{53}$$

So combining Eqs. (39) and (53) yields

$$\begin{bmatrix} y \\ y_1 \end{bmatrix} = \begin{bmatrix} C \\ C_1 \end{bmatrix} x \tag{54}$$

which can be solved to obtain

$$x = \begin{bmatrix} C \\ C_1 \end{bmatrix}^{-1} \begin{bmatrix} y \\ y_1 \end{bmatrix} = \begin{bmatrix} F & F_1 \end{bmatrix} \begin{bmatrix} y \\ y_1 \end{bmatrix} = Fy + F_1 y_1 \tag{55}$$

An estimate of x can be obtained from Eq. (55) as

$$\hat{x} = Fy + F_1 \hat{y}_1 \tag{56}$$

where y is a known system measurement and y_1 is to be determined from the reduced-order observer of dimension r.

From Eq. (55), one can obtain

$$\begin{aligned} \begin{bmatrix} C \\ C_1 \end{bmatrix} \begin{bmatrix} C \\ C_1 \end{bmatrix}^{-1} = I_n &= \begin{bmatrix} C \\ C_1 \end{bmatrix} \begin{bmatrix} F & F_1 \end{bmatrix} \\ &= \begin{bmatrix} CF & CF_1 \\ C_1 F & C_1 F_1 \end{bmatrix} \\ &= \begin{bmatrix} I_p & 0 \\ 0 & I_r \end{bmatrix} \end{aligned} \tag{57}$$

where I_n is an identity matrix of order n. From Eq. (57), $C_1 F = CF_1 = 0$, $CF = I_p$ and $C_1 F_1 = I_r$.

Now, from Eq. (53), the differential equation for y_1 can be obtained as

$$\dot{y}_1 = C_1 AFy + C_1 AF_1 y_1 + C_1 Bu \tag{58}$$

However, y does not contain information about y_1, because

$$y = Cx = CFy + CF_1 y_1 = y + 0 \tag{59}$$

Nevertheless, more information about y_1 from $\dot{y}$ is obtained as follows

$$\dot{y} = CAFy + CAF_1 y_1 + CBu \tag{60}$$

This indicates that $\dot{y}$ contains information about y_1. Therefore, an observer for y_1 is constructed as

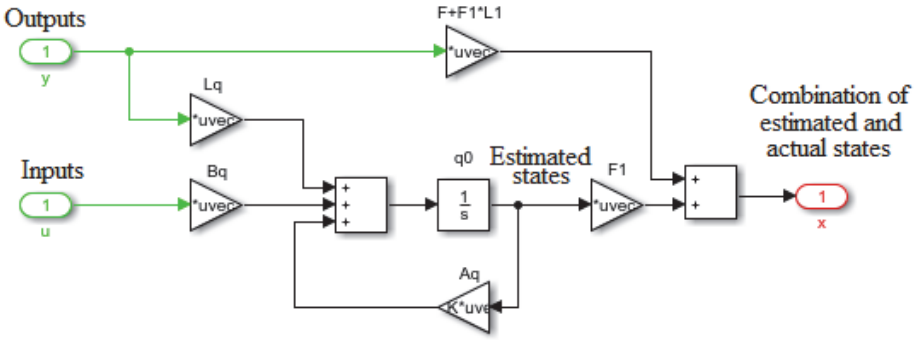

Fig. 3: Simulink block diagram of state estimation using a reduced-order observer.

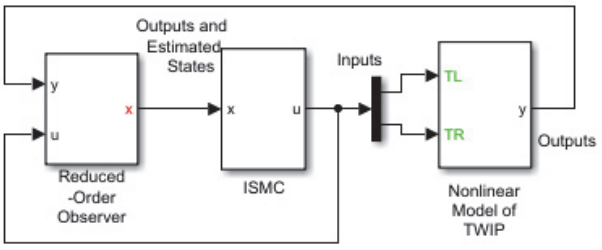

Fig. 4: Overall Simulink block diagram of the control scheme.

$$\dot{\hat{y}}_1 = C_1AFy + C_1AF_1\hat{y}_1 + C_1Bu + L_1(\dot{y} - \dot{\hat{y}}) \quad (61)$$

where L_1 is the reduced-order observer gain, which has to be determined so that the reduced-order observation error $(\dot{y} - \dot{\hat{y}})$ goes to zero. In this, $\dot{\hat{y}}$ is obtained from Eq. (60) as

$$\dot{\hat{y}} = CAFy + CAF_1\hat{y}_1 + CBu \quad (62)$$

Substituting Eq. (62) into Eq. (61) and defining $\hat{q} = \hat{y}_1 - L_1y \rightarrow \dot{\hat{q}} = \dot{\hat{y}}_1 - L_1\dot{y}$, the reduced-order observer for $\hat{q}$ is obtained as

$$\dot{\hat{q}} = A_q\hat{q} + B_qu + L_qy \quad (63)$$

where $A_q = \left(C_1 - L_1C\right)AF_1$, $B_q = \left(C_1 - L_1C\right)B$, and $L_q = \left(C_1 - L_1C\right)A\left(F - F_1L_1\right)$.

Using observation for $\hat{q}$ the reduced-order observer is obtained for $\hat{y}_1$ as

$$\hat{y}_1 = \hat{q} + L_1y \quad (64)$$

which gives the estimate for original state x in Eq. (45) as

$$\hat{x} = (F + F_1L_1)y + F_1\hat{q} \quad (65)$$

The state estimation for the system Eq. (44) depicted in Fig. 3 is in the form of a block diagram using Eq. (65). For this state estimation, the control input (u) (from Fig. 2) and system outputs (y) (from Fig. 1) are used as inputs. The output of the block diagram in Fig. 3, i.e., a combination of the actual and estimated states is then connected with states in Fig. 2 to generate a control signal. Figs. 1, 2, and 3 are combined in Fig. 4 to form an overall simulation block diagram of the TWIP system with an observer-based integral sliding mode controller. The parameter values and other calculated values are run in the script file and stored in the MATLAB workspace. These values are fetched by the Simulink model.

5. SIMULATION RESULTS AND DISCUSSIONS

Initially, the state feedback gain matrix is determined for the linear TWIP system, as given in Eq. (45), to place the eigenvalues at $(-6, -4.5, -3\pm0.5i, -1.5\pm0.25i)$. The discontinuous control signal Eq. (50) is then formulated with $\mu = 2$ and $k = 3$. Next, the total control input Eq. (52) is constructed using Eqs. (45) and (50). This ISMC signal requires outputs and estimated states. These are obtained from a reduced-order observer as per the procedure given in Section 4. The observer poles are placed at $(-20, -18, -16)$, and the complete closed-loop system is simulated with the nonlinear model of the TWIP. The initial conditions for the nonlinear model of the TWIP are arbitrarily selected as (0.1, 0, 0.2, 0, 0.3, 0) for checking the regulation performance. The initial conditions for the reduced-order observer are calculated according to [23].

Initially, the performance of the reduced-order observer is checked by plotting the estimation errors for the immeasurable states (x_2, x_4, x_6) as depicted in Fig. 5. The estimation error is calculated as $e = x - \hat{x}$ for all the states, where x is the actual state and $\hat{x}$ is an estimated state. From Fig. 5, it can be observed that the estimation errors reach zero in less than 2 s. This indicates that the reduced-order observer estimates the immeasurable states with good accuracy. In all other simulation experiments, the estimated states are given to the controller and the results are generated. Various cases of the simulation are explained as follows.

The regulation performance with ISMC is observed

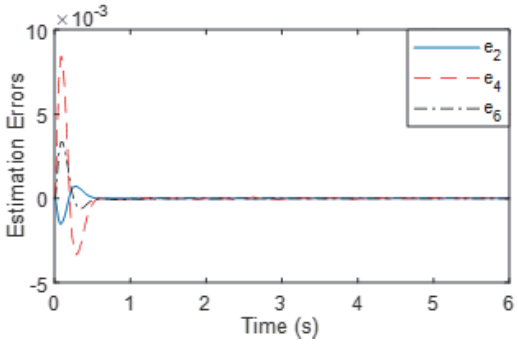

Fig. 5: Estimation errors for x_2, x_4, x_6.

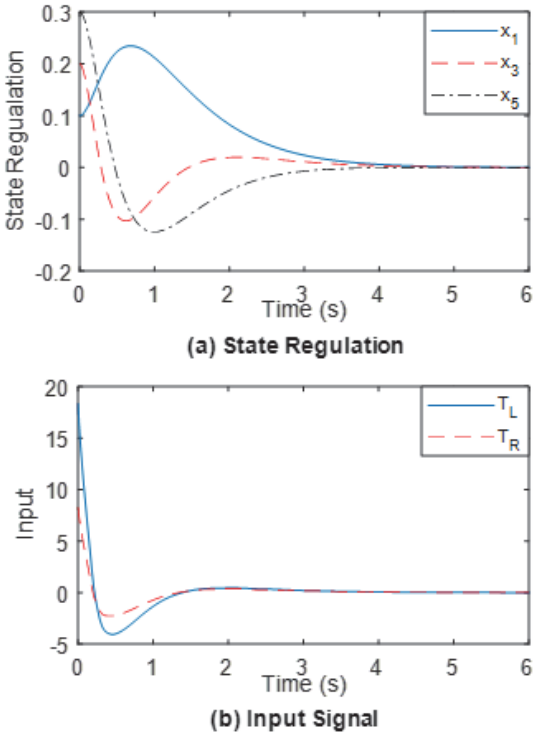

Fig. 6: Regulation response of the system.

under the initial conditions illustrated in Fig. 6. According to Fig. 6(a), all the outputs are regulated and attain a steady state within 5 s. Fig. 6(b) shows the responses of input signals. Here the inputs also attain a steady state in less than 2 s. The regulation response is found to be satisfactory, despite not being plotted for the immeasurable states, as evidenced by the estimation errors in Fig. 5. The estimation error is also observed to be very small.

The second simulation experiment is conducted with continuous disturbance applied to both wheels. The disturbance applied to the left wheel is $d_L = 0.3\sin(t)$ and $d_R = 0.3\cos(t)$ to the right wheel. Accordingly, the responses are obtained as shown in Fig. 7. In this, the performance is compared with the linear quadratic regulator, since they both have the same feedback gain matrix. As can be observed from Fig. 7, the response with

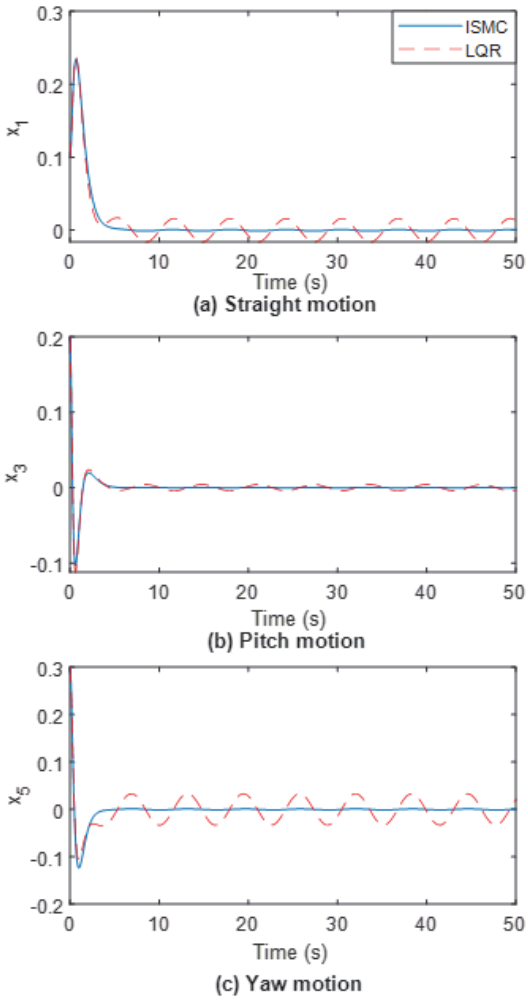

Fig. 7: Response to continuous disturbance.

Table 2: Comparison of error performance indices for continuous disturbance.

Error Indices	Control	x_1	x_3	x_5
ITSE	ISMC	0.060	0.005	0.018
	LQR	0.225	0.017	0.700
ITAE	ISMC	1.300	0.350	1.240
	LQR	13.00	3.400	27.00

the simple LQR is oscillatory with a constant frequency and steady for the proposed ISMC. It must be noted that even for LQR the estimated states are used for a fair comparison of controllers.

The graphs in Fig. 7 are also compared based on the error performance indices, namely integral time square error (ITSE) and integral time absolute error (ITAE), as shown in Table 2, calculated for outputs x_1, x_3, and x_5. Table 2 shows that the performance with ISMC is much better than for LQR.

In the third simulation, the constant disturbance $d = 0.3$ N of the short interval (20 s) is applied to the left

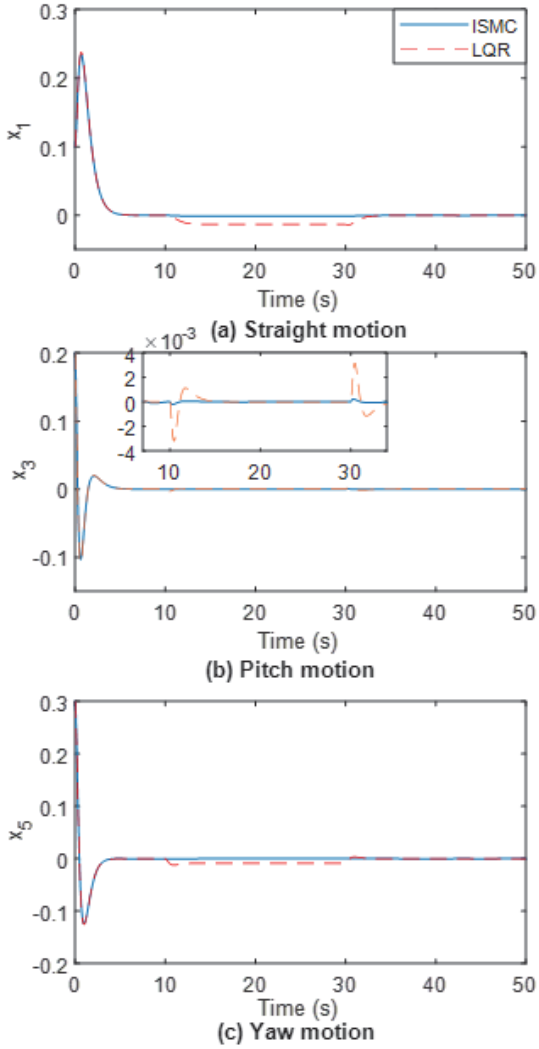

***Fig. 8**: Response to constant disturbance.*

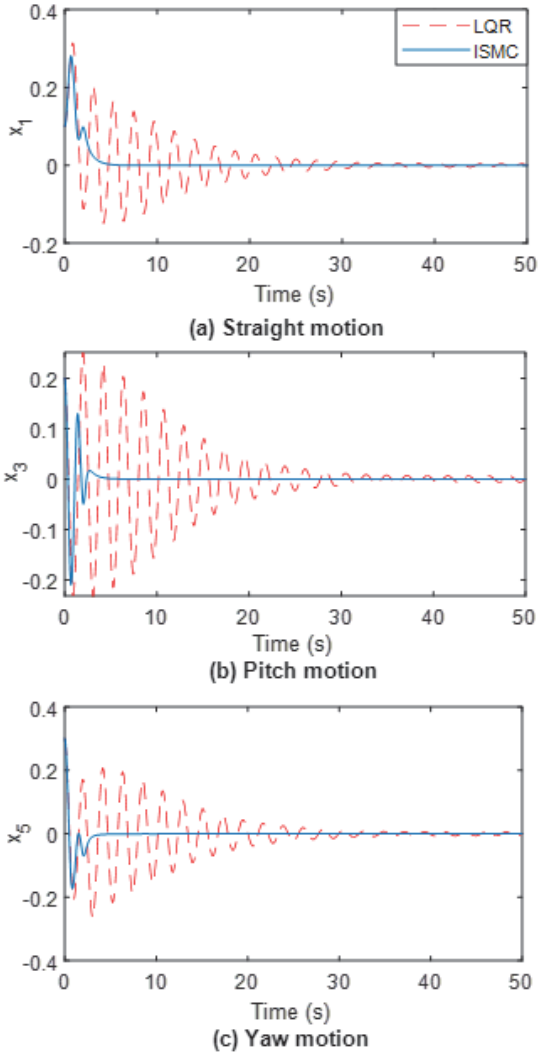

***Fig. 9**: Response to the parameter variations.*

***Table 3**: Comparison of error performance indices for constant disturbance.*

Error Indices	Control	x_1	x_3	x_5
ITSE	ISMC	0.060	0.005	0.018
	LQR	0.130	0.006	0.050
ITAE	ISMC	0.900	0.150	0.280
	LQR	6.200	0.310	4.000

***Table 4**: Comparison of error performance indices for parameter variations.*

Error Indices	Control	x_1	x_3	x_5
ITSE	ISMC	0.055	0.021	0.019
	LQR	0.640	1.100	1.100
ITAE	ISMC	0.480	0.250	0.240
	LQR	10.00	13.00	14.00

wheel. The disturbance is applied at 10 s and removed at 30 s. The response is plotted in Fig. 8 and compared with LQR. Here, the performance of ISMC is also found to be unaffected. In a system with LQR, small variations at the start of disturbance and the time of its removal can be observed. In fact, with LQR for straight and yaw motions, there are steady-state errors of 0.02 and 0.01, respectively. Again, the results are compared between ITSE and ITAE as shown in Table 3. This shows that the performance of the proposed ISMC is robust.

In the final simulation, parameter variation is considered, whereby all the parameters of the system listed in Table 1 are changed slowly. It can be observed that after a 45% change in parameters, the performance with the LQR becomes unstable. Hence, all the parameters are increased by 45% and the responses plotted as shown in Fig. 9.

As can be observed, the performance of the proposed ISMC is much better than the LQR. The system with LQR oscillates up to 30 s and then settles. However, the system with ISMC does not show oscillations like

LQR. Comparing the settling time of responses between LQR and ISMC, a five-fold improvement is achieved with ISMC. In addition, the values of ITSE and ITAE are determined for output and compared in Table 4.

In all simulation cases, it can be observed that the performance of the proposed ISMC is superior to the LQR for constant and time-varying disturbances and parameter variations.

Undoubtedly, the performance of the proposed ISMC with the suggested reduced-order observer is found to be superior to LQR. However, it depends heavily on the location of poles for the controller and observer and the controller parameters such as μ and k. In this paper, a generalized approach is used with no specific procedure suggested for the selection of poles and controller parameters. Furthermore, the selection can be verified by real system simulation.

6. CONCLUSION

In this paper, a reduced-order observer-based integral sliding mode control technique is proposed for the two-wheeled inverted pendulum system. First, the modeling of the TWIP system is discussed with the MATLAB Simulink blocks. The integral sliding mode controller is then designed. The ISMC realization requires all the states, hence immeasurable states are estimated using a reduced-order observer. MATLAB Simulink block diagrams for the controller and observer are also presented. This scheme is then tested with continuous and constant disturbances as well as parameter variations. The results are compared with the LQR. According to the simulation studies, the proposed ISMC is found to result in zero steady-state error in the presence of disturbance with a five-fold improvement in settling time for parameter variations. Future work should involve the development of system hardware.

REFERENCES

[1] A. Castro, "Modeling and dynamic analysis of a two-wheeled inverted pendulum," M.S. thesis, School of Mechanical Engineering, Georgia Institute of Technology, Atlanta, Georgia, USA, 2012.

[2] S. Kim and S. Kwon, "Dynamic modeling of a two-wheeled inverted pendulum balancing mobile robot," *International Journal of Control, Automation and Systems*, vol. 13, no. 4, pp. 926–933, Aug. 2015.

[3] C. Xu, M. Li, and F. Pan, "The system design and LQR control of a two-wheels self-balancing mobile robot," in *2011 International Conference on Electrical and Control Engineering*, Yichang, China, 2011, pp. 2786–2789.

[4] M. Muhammad, S. Buyamin, M. N. Ahmad, S. W. Nawawi, and Z. Ibrahim, "Velocity tracking control of a two-wheeled inverted pendulum robot: a comparative assessment between partial feedback linearization and LQR control schemes," *International Review on Modelling and Simulations*, vol. 5, no. 2, pp. 1038–1048, Apr. 2012.

[5] C.-H. Huang, W.-J. Wang, and C.-H. Chiu, "Design and implementation of fuzzy control on a two-wheel inverted pendulum," *IEEE Transactions on Industrial Electronics*, vol. 58, no. 7, pp. 2988–3001, Jul. 2011.

[6] M. Muhammad, S. Buyamin, M. N. Ahmad, and S. W. Nawawi, "Takagi-Sugeno fuzzy modeling of a two-wheeled inverted pendulum robot," *Journal of Intelligent & Fuzzy Systems: Applications in Engineering and Technology*, vol. 25, no. 3, pp. 535–546, May 2013.

[7] J.-X. Xu, Z.-Q. Guo, and T. H. Lee, "Design and implementation of integral sliding-mode control on an underactuated two-wheeled mobile robot," *IEEE Transactions on Industrial Electronics*, vol. 61, no. 7, pp. 3671–3681, Jul. 2014.

[8] S. Kim and S. Kwon, "Nonlinear optimal control design for underactuated two-wheeled inverted pendulum mobile platform," *IEEE/ASME Transactions on Mechatronics*, vol. 22, no. 6, pp. 2803–2808, Dec. 2017.

[9] H. F. Murcia and A. E. González, "Performance comparison between PID and LQR control on a 2-wheel inverted pendulum robot," in *2016 IEEE Colombian Conference on Robotics and Automation (CCRA)*, Bogota, Colombia, 2016.

[10] K. Prakash and K. Thomas, "Study of controllers for a two wheeled self-balancing robot," in *2016 International Conference on Next Generation Intelligent Systems (ICNGIS)*, Kottayam, India, 2016.

[11] H. S. Zad, A. Ulasyar, A. Zohaib, and S. S. Hussain, "Optimal controller design for self-balancing two-wheeled robot system," in *2016 International Conference on Frontiers of Information Technology (FIT)*, Islamabad, Pakistan, 2016, pp. 11–16.

[12] B. Shilpa, V. Indu, and S. R. Rajasree, "Design of an underactuated self balancing robot using linear quadratic regulator and integral sliding mode controller," in *2017 International Conference on Circuit, Power and Computing Technologies (ICCPCT)*, Kollam, India, 2017.

[13] S. Wenxia and C. Wei, "Simulation and debugging of LQR control for two-wheeled self-balanced robot," in *2017 Chinese Automation Congress (CAC)*, Jinan, China, 2017, pp. 2391–2395.

[14] N. Uddin, T. A. Nugroho, and W. A. Pramudito, "Stabilizing two-wheeled robot using linear quadratic regulator and states estimation," in *2017 2nd International conferences on Information Technology, Information Systems and Electrical Engineering (ICITISEE)*, Yogyakarta, Indonesia, 2017, pp. 229–234.

[15] L. Pupek and R. Dubay, "Velocity and position trajectory tracking through sliding mode control of two-wheeled self-balancing mobile robot," in *2018 Annual IEEE International Systems Conference (SysCon)*, Vancouver, British Columbia, Canada, 2018.

[16] H. Al-Jlailaty, H. Jomaa, N. Daher, and D. As-

mar, "Balancing a two-wheeled mobile robot using adaptive control," in *2018 IEEE International Multidisciplinary Conference on Engineering Technology (IMCET)*, Beirut, Lebanon, 2018.

[17] M. A. Imtiaz, M. Naveed, N. Bibi, S. Aziz, and S. Z. H. Naqvi, "Control system design, analysis & implementation of two wheeled self balancing robot (TWSBR)," in *2018 IEEE 9th Annual Information Technology, Electronics and Mobile Communication Conference (IEMCON)*, Vancouver, British Columbia, Canada, 2018, pp. 431–437.

[18] Y. Boucetta, R. Ayad, and Z. Ahmed-Foitih, "Control of mobile robot using fractional order $PI^{\lambda}D^{\mu}$ controller," *ECTI Transactions on Electrical Engineering, Electronics, and Communications*, vol. 17, no. 2, pp. 144–151, Aug. 2019.

[19] N. Hasanah, A. H. Alasiry, and B. Sumantri, "Two wheels line following balancing robot control using fuzzy logic and PID on sloping surface," in *2018 International Electronics Symposium on Engineering Technology and Applications (IES-ETA)*, Bali, Indonesia, 2018, pp. 210–215.

[20] *MATLAB: Simulink Control Design Toolbox User Manual, Version 4.5*, MathWorks, 2017.

[21] P. V. Surjagade, A. P. Tiwari, and S. R. Shimjith, "Robust optimal integral sliding mode controller for total power control of large PHWRs," *IEEE Transactions on Nuclear Science*, vol. 65, no. 7, pp. 1331–1344, Jul. 2018.

[22] R. J. Desai, B. M. Patre, R. K. Munje, A. P. Tiwari, and S. R. Shimjith, "Integral sliding mode for power distribution control of advanced heavy water reactor," *IEEE Transactions on Nuclear Science*, vol. 67, no. 6, pp. 1076–1085, Jun. 2020.

[23] W. Gao and J. Hung, "Variable structure control of nonlinear systems: a new approach," *IEEE Transactions on Industrial Electronics*, vol. 40, no. 1, pp. 45–55, Feb. 1993.

[24] V. Radisavljevic-Gajic, "Full- and reduced-order linear observer implementations in Matlab/Simulink," *IEEE Control Systems Magazine*, vol. 35, no. 5, pp. 91–101, Oct. 2015.

Ravindra Munje received B.E. degree in Electrical from Mumbai University, Mumbai, India in 2005, M.E. degree in Electrical (control systems) from Pune University, Nashik, India in 2009, and Ph.D. Degree in Electrical from Swami Ramanand Teerth Marathwada University, Nanded, India in 2015. He was a Post-Doctoral Fellow with Shanghai Jiao Tong University, Shanghai from June 2017 to May 2019. Currently, he is a Professor at the Electrical Engineering Department, K. K. Wagh Institute of Engineering Education and Research, Nashik, India. He has written a book and about 50 refereed papers. His research interests include modeling and control of large-scale systems using sliding mode, multirate output feedback, and power quality analysis using AI techniques.

Dr. Munje received the Promising Engineer Award in 2016, Outstanding Researcher Award in 2018 and Best Faculty Award in 2019.

Ranvir J. Desai received his Bachelor's degree and Master's degree in Instrumentation Engineering from Shri Guru Gobind Singhji (SGGS) Institute of Engineering and Technology, Nanded, India in 2017. Currently, he is working as a Senior Research Fellow under Board of Research in Nuclear Sciences (BRNS) sponsored project at SGGS Institute of Engineering and Technology, Nanded, India. and pursuing a Ph.D. in nuclear reactor control and estimation from Swami Ramanand Teerth Marathwada University, Nanded, India. He has published 2 research papers in international journals and presented 1 at an international conference. His areas of interest are modern control theory, robust control, process control, optimal estimation and nuclear reactor control.

Balasaheb M. Patre received his Bachelor of Instrumentation Engineering in 1986, Masters of Instrumentation Engineering in 1990, both from Shri Guru Gobind Singhji (SGGS) Institute of Engineering and Technology, Vishnupuri, Nanded, India and Ph.D. from Indian Institute of Technology Bombay, India in 1998. Currently, he is working as a Professor at the Department of Instrumentation Engineering, SGGS Institute of Engineering and Technology, Nanded, India. He has published more than 80 international journal papers, more than 100 national and international conference papers, 6 books and 5 book chapters. He is a reviewer for 45 international (SCI/SCIE indexed) peer-reviewed journals. He has completed sponsored research projects from DST, AICTE, BARC, BRNS and NRB. He has so far supervised 22 students for Ph.D. and 5 students are currently pursuing Ph.D. under his guidance in the areas of systems and control engineering in general and robust control, nuclear reactor control, sliding mode control and applications, and process control in particular.

Dr. Patre is a senior member of IEEE, a Fellow of the Institution of Engineers (India), a Member of IETE (India) and a life member of ISTE.